An Analysis of elastic and inelastic lateral torsional buckling of web-tapered I beams using the finite element method

Paulus Karta Wijaya[1,*], *Cecilia* Lauw Giok Swan[1], and *Ghassani* Sadrina Noor[2]

[1]Universitas Katolik Parahyangan, Civil Engineering Department, Bandung, Indonesia
[2]Waskita Karya, Jakarta, Indonesia

Abstract. Elastic and inelastic lateral torsional buckling of simply web tapered I beam is studied using the finite element method. The length of the beams is 8000 mm for elastic lateral torsional buckling and 4000 mm for inelastic lateral torsional buckling. The depth of cross section at one end is 500 mm and at the other end it is varied. The thickness of the flange is 16 mm and the thickness of the web is 10 mm. The section of the beams is compact. The beams are loaded by end moments. The ratio of end moments at one end and the moments at the other end are varied. The beams are assumed to have geometric imperfection and the distribution of imperfection follows the shape of the first buckling mode of elastic lateral torsional buckling of the beam. The amplitude of the imperfection is taken one milimeter at the top flange in lateral direction. The load is increased until the beams collapse. The ultimate load is considered as the critical moments of the beams. The results of the analysis are compared to nominal lateral torsional buckling moments using the method presented in the AISC Design Guide 25 (Design Guide for web tapered members). It can be concluded that usually the critical moments of the collapse analysis are close to the critical moments of the design guide. But sometimes it is less than the design guide and it means design guide is sometimes is not on the safe side.

1 Introduction

Web tapered steel beams are usually used due to economic aspects. In beam design, one of the consideration is lateral torsional buckling. Study of lateral torsional buckling of web tapered I beams has been made by many researchers. Polyzois [1] studied the modification factor using FEM. The analysis consists of the elastic buckling analysis. Miller [2] studied lateral torsional buckling of web tapered I beams using non-linear finite element method. J.S Park et al [3] studied lateral torsional buckling of stepped beams using the linear finite element method. Vandermeulen et al [4] studied lateral torsional buckling of tapered beams using the linear and nonlinear finite element method, but residual stress was not considered. Zhang and Tong [5] developed a new theory for lateral torsional buckling of web tapered I beams. They formulated total potential energy for lateral torsional buckling of elastic I beams and used the classical variational principle for buckling analysis. Raftoyiannis and Adamakos [6] developed a simple numerical approach for determining elastic critical lateral torsional buckling. Kovac,M. [7] studied elastic lateral torsional buckling of web tapered I beams using the 1D and 3D FEM method. He developed the 1D element and compared it to the 3D shell element model. Naaim et al [8] studied lateral torsional buckling behaviour of the web tapered section with perforation using the finite element method. Patil [9] studied lateral torsional buckling of web tapered cantilever beams using the finite element method.

This paper presents the results of a study about lateral torsional buckling of web tapered I beams loaded by end moments. The cross section of the beam is the compact section. The method of analysis is the finite element method. The beam, modelled by the finite element method, is loaded by incremental load until they collapse. For the buckling analysis, geometric imperfection of the beams must be introduced. The residual stress is taken into account. The results of analysis are compared with the critical moment computed using the AISC Steel Design Guide 25.

2 AISC Design Guide 25

The AISC Design Guide 25 (DG 25) [10] provides a method to design web tapered members. In the design guide, there is a method to evaluate the lateral torsional buckling strength of tapered beams. The procedure is

* Corresponding author: paulusk@unpar.ac.id

presented briefly in this paper and the result of using this design guide will be compared to the result of the finite element analysis. The method of DG 25 presented here is only for doubly symmetric and compact sections.

First elastic lateral torsional buckling stress, F_{eLTB}, is calculated using equation (1) and section properties at the middle of the unbraced length.

$$F_{eLTB} = \frac{\pi^2 E}{(L_b / r_t)^2}\sqrt{1 + 0.078\frac{J}{S_x h_o}\left(\frac{L_b}{r_t}\right)^2} \qquad (1)$$

E stands for the modulus of elasticity, L_b is unbraced length, r_t is effective radius gyration for lateral torsional buckling, J is torsional constant, S_x is section modulus about strong axis, h_o is distance between flange centroids.

Determine the location of maximum compressive flexural stress, $f_{r\max}$, within the unbraced length. At this location, calculate the nominal buckling stress multiplier, γ_{eLTB} which is equal to $F_{eLTB}/f_{r\max}$. Calculate the nominal moment, M_n, at various location along the unbraced length using the following equation

If $\frac{(\gamma_{eLTB})f_r}{F_y} \geq \frac{\pi^2}{1.1} = 8.2$ the lateral torsional buckling limit state does not apply.

If $8.2 \succ \frac{(\gamma_{eLTB})f_r}{F_y} \geq 0.7$ calculate the nominal lateral torsional buckling strength

$$M_n = M_p - 0.3767(M_p - 0.7F_y S_x)\left(\pi\sqrt{\frac{F_y}{(\gamma_{eLTB})f_r}} - 1.1\right) \qquad (2)$$

If $\frac{(\gamma_{eLTB})f_r}{F_y} \prec 0.7$

$$M_n = C_b(\gamma_{eLTB})f_r S_x \qquad (3)$$

C_b is the lateral torsional buckling modification factor for nonuniform moment diagram, f_r is flexural stress at the location considered.

3 Problem statement

The problem considered is a simply supported beam as illustrated in Figure 1. The beam is web tapered. Torsional rotation at the ends of the beam is restrained but warping is allowed. The loads are end moments. The bending moment in the beam is a positive single curvature (upper flange is in compression). The ratio between the right end moment to the left end moment is varied.

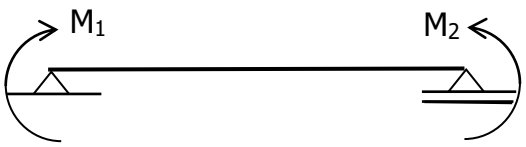

Fig. 1. The beam considered.

3 Finite element model

3.1. Geometrical model

The beam is modelled by shell element as is illustrated in Fig.2. The element is four node element with six degrees of freedom per node, three translations and three rotations. A Cartesian coordinate is shown in the figure. At one end of the beam, the node at centroid is restrained in three translation directions and the other nodes are free at x direction and restrained at y and z directions. At the other end of the beam, all nodes are restrained at y and z directions and free at x direction. These boundary conditions are used to accommodate warping at the boundary.

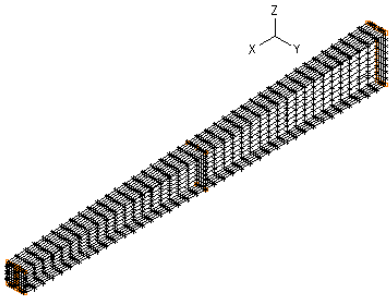

Fig. 2. Finite element model of a web-tapered beam

3.2. Material model

The material is modelled as a plastic multi linier material model. Yield stress, F_y, is 250 MPa and the tensile strength is 410 MPa. The stress-strain relation is modelled as piecewise linear as shown in Figure 3.

Residual stress is taken into account. Distribution of the residual stress is linear and the maximum residual stress is 0,3 yield stress as shown in Fig. 4. In the finite element analysis the section element is divided into 8 parts for the flange and 8 parts for the web. Residual stress is modelled as constant at each part as shown at Fig. 5. To take into account the residual stress, the yield stress and tensile strength are superposed according the stress due to loading. Due to loading, the top flange is in compression, the yield stress for each part is modified by substracting yield stress of the material by the residual stress at each part. For the bottom flange, the yield stress of each part is modified by adding yield stress of the material by residual stress of each part.

3.3. Loading model

The end moments are modelled as point loads at nodes at flanges and at the end of the beam. The loads at the upper flanges are the same in magnitude but in opposite direction of the load at the lower flanges. The end moment is the total load at the upper flange multiplied by the distance between flange centroids. The ratio of the right end moment to the left end moment is varied.

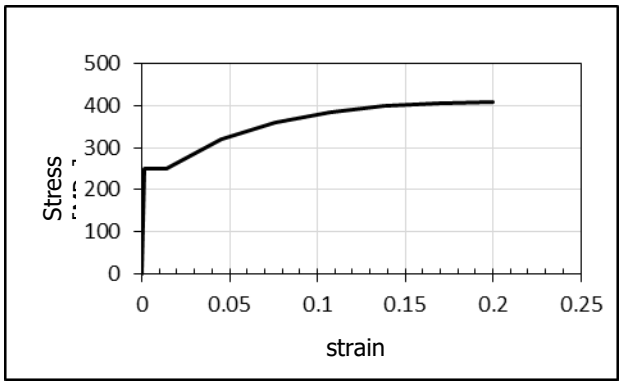

Fig. 3. Stress – strain diagram used in the analysis.

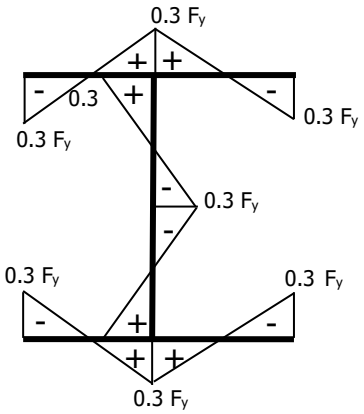

Fig. 4. Residual stress distribution.

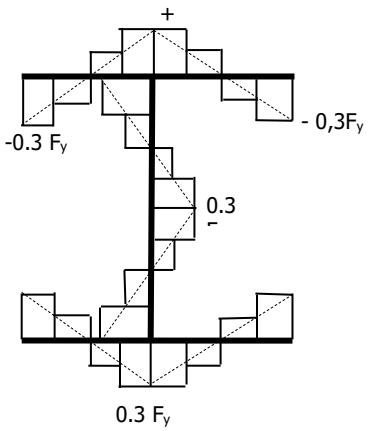

Fig. 5. Model of residual stress for finite element analysis.

4 Collapse analysis

The analysis consists of the nonlinear incremental load method and is called collapse analysis. The analysis is performed using the ADINA program. In collapse analysis, the structure is given displacement control loading. The nodal displacement at the loaded nodes are increased gradually with small increments and the nodal forces are computed for each step until the beam collapses. For buckling analysis, before the collapse analysis is performed, the beam is given geometric imperfection. The shape of distribution of geometric imperfection is taken as the first buckling mode computed by the linear buckling analysis. Linear buckling analysis is the Eigen value buckling analysis. The amplitude of imperfection is taken to be 1 mm in lateral direction at the middle of the top flange. After the analysis, nodal load - lateral deflection curve will be obtained. The maximum load is interpreted as the critical load of the beam. Figure 6 shows the shape of deformation after the collapse analysis is completed.

5 Verification of finite element method

Two prismatic beams are analysed using collapse analysis for verification of the method. The length of the first beam is 8000 mm and the length of the second one is 4000 mm. Both of the beams are WF500x200x10x16. Figure 6 shows the displacement of the beam with an 8000 span at the end of analysis. Figure 7 shows the curve of nodal load versus lateral displacement at the middle of top flange the beam with an 8000 mm span and Figure 8 shows the curve for beam with a 4000 mm span. In Figure 7 and Figure 8, the load is the load at one loaded node. The maximum load is considered as the critical load and the critical moment is computed using this critical load.

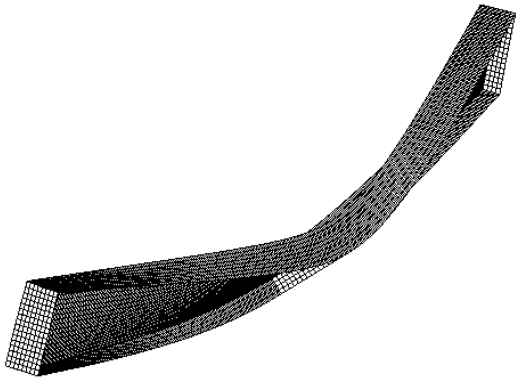

Fig. 6. Displacement of the beam at the end of collapse analysis.

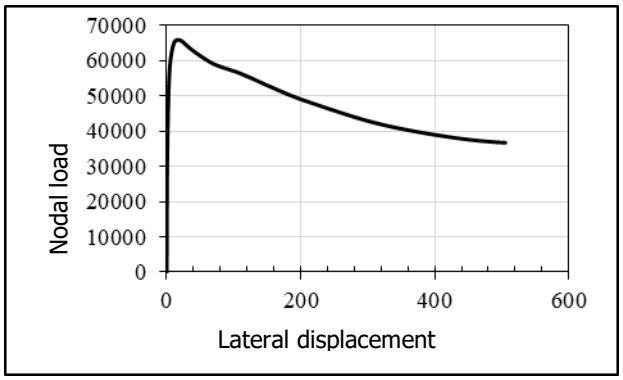

Fig. 7. Nodal load vs lateral nodal displacement at the middle of the top flange of the prismatic beam with 8000 mm span

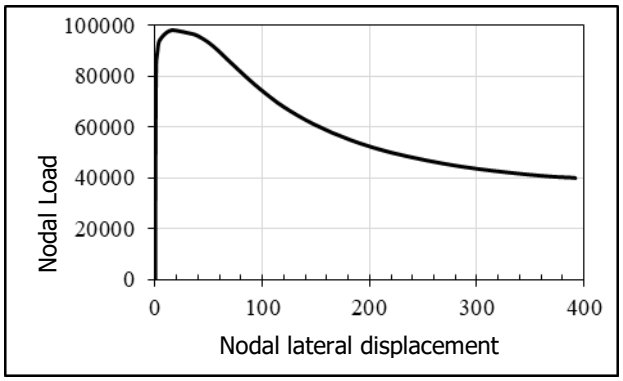

Fig. 8. Nodal load vs lateral nodal displacement at the middle of the top flange of the prismatic beam with 4000 mm span.

Table 3. M_{cr} elastic analytical vs M_{cr} elastic finite element.

L	M_{cr} elastic	M_{cr} elastic FEM	difference
8000	247854.7 N-m	268794.2 N-m	8.45%
4000	742887.0 N-m	698508.8 N-m	-5.97%

Table 4. M_{cr} AISC vs M_{cr} collapse analysis.

L	M_{cr} AISC	M_{cr} inelast FEM	difference
8000	247854.7 N-m	254417.1 N-m	2.65%
4000	444026.58 N-m	379810 N-m	-14.46%

In Table 3, the elastic critical moment computed by linear buckling FEM (finite element method) is compared to the analytical critical moment. The difference is 8.45% for 8000 mm span beam and -5.97% for 4000 mm beam. The difference is below 10%. It can be concluded that the result for linear buckling has sufficiently converged.

In Table 4 the critical moment computed from the collapse analysis is compared to the nominal moment from the AISC equations. The difference is 2.65% for 8000 mm beam and -14.46% for 4000 mm beam. For the long beam the failure is elastic buckling and the AISC formula for this is an exact solution of the differential equation and the result of collapse analysis is very good. For the 4000 mm beam, the difference is -14,46% but the AISC formula for this is not an exact solution, so it cannot be used as verification. From Table 3 and 4, it is concluded that the model for collapse analysis can be used for buckling analysis.

5 Result of analysis

There are two series of beams. The span of the first beam is 8000 mm and the span of the second beam is 4000 mm. The depth of the left end cross section is 500 mm and the right end cross section is varied. The flange width is 200 mm, the thickness of the flange is 16 mm and the thickness of the web is 10 mm. Left end moment is M_1 and right end moment is M_2. The ratio of end moments M_2/M_1 is varied. The name of the beam model with the right depth end cross section and ratio of the end moments is shown at Table 3 for beams with an 8 meter span and Table 4 for beams with is a 4 meter span.

Table 3. Beams with 8000 mm span.

Name of beam	Right depth (mm)	M_2/M_1
1-A-1	400	1
1-A-2	400	4/5
1-A-3	400	3/5
1-A-4	400	1/2
1-A-5	400	0
1-B-1	300	1
1-B-2	300	4/5
1-B-3	300	3/5
1-B-4	300	1/2
1-B-5	300	0
1-C-1	200	1
1-C-2	200	4/5
1-C-3	200	3/5
1-C-4	200	1/2
1-C-5	200	0

Table 4. Beams 4000 mm length.

Name of beam	Right depth	m/M
2-A-1	400	1
2-A-2	400	4/5
2-A-3	400	3/5
2-A-4	400	1/2
2-A-5	400	0
2-B-1	300	1
2-B-2	300	4/5
2-B-3	300	3/5
2-B-4	300	1/2
2-B-5	300	0
2-C-1	200	1
2-C-2	200	4/5
2-C-3	200	3/5
2-C-4	200	1/2
2-C-5	200	0

After collapse analysis is completed, the load-displacement curve can be drawn.

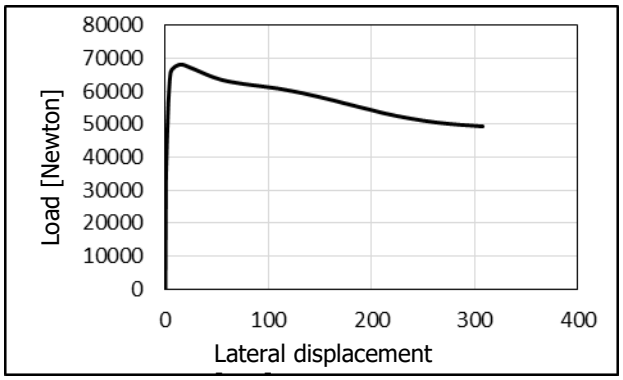

Fig. 9. Nodal load at a node at the end of the beam vs lateral displacement at the middle of the top flange of the 1-C-4 beam.

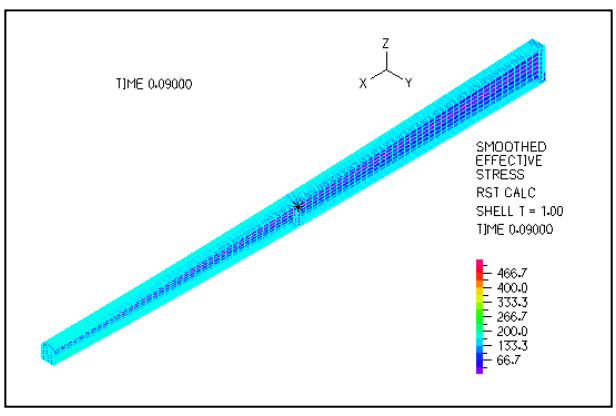

Fig. 10. Stress distribution of the 1-C-4 beam at the peak load (stress in MPa)

Figure 9 shows the nodal load at the end of the beam versus lateral displacement at the middle of the top flange of beam 1-C-4. The peak load is 65827.2 N, occurred at y displacement 13.7 mm

Figure 10 shows stress distribution in beam 1-C-4 at the peak load. It can be seen that the stress is in the elastic range. It confirms that the use of elastic buckling formula is correct.

Figure 11 shows the nodal load at the end of the beam versus lateral displacement at the middle of top flange for beam 2-C-4. The peak load is 91093 N, occurred at a y displacement of 22.93 mm.

It is interesting to observe that lateral displacement for the 8 meter beam is smaller than for the 4 meter beam at their peak load.

Figure 12 shows stress distribution in beam 2-C-4 at the peak load. It can be seen that at the flange the stress is in inelastic range and the web is still in elastic range.

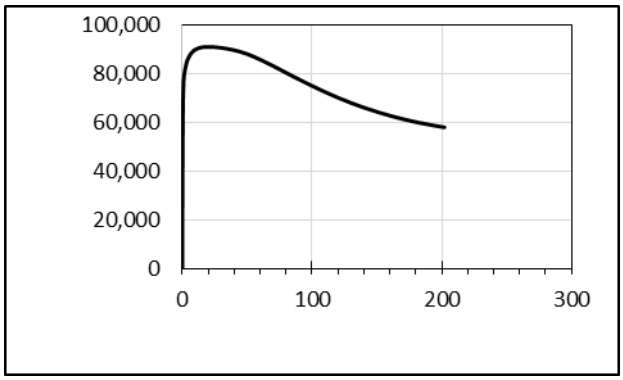

Fig. 11. Nodal load at the end of the beam vs lateral displacement at the middle of the top flange of the 2-C-4 beam.

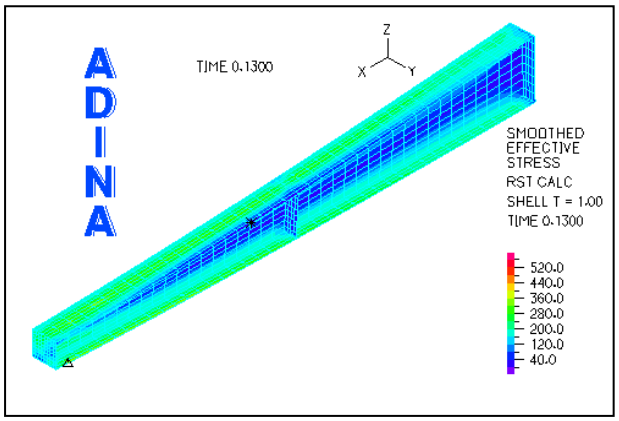

Fig. 12. Stress distribution of the 2-C-4 beam at the peak load

The results of all analyses are tabulated in Table 5 for beams with an 8000 mm span and Table 6 for beams with a 4000 mm span. The Tables also show the difference between the critical moment from collapse analysis and DG-25.

Table 5. Analysis result of beams with an 8000 mm span

Beam	End moment Ratio	Collapse	DG-25	Difference [%]
1-A-1	1	230462400	238079609	3.3
1-A-2	0.8	256316800	257992082	0.7
1-A-3	0.6	287596800	289413623	0.6
1-A-4	0.5	305527600	307297656	0.6
1-A-5	0	394435600	466586941	18.3
1-B-1	1	213843600	196712044	-8.0
1-B-2	0.8	250683200	228350469	-8.9
1-B-3	0.6	276210400	271386705	-1.7
1-B-4	0.5	293778000	298498517	1.6
1-B-5	0	382925600	420322501	9.7
1-C-1	1	185008000	158696402	-14.2
1-C-2	0.8	216705200	188852495	-12.9
1-C-3	0.6	252602000	232262157	-8.1
1-C-4	0.5	272165600	260017822	-4.5
1-C-5	0	368044000	420390179	14.2

Table 6. Analysis result of beams with a 4000 mm span

Beam	End moment Ratio	Collapse	DG-25	Difference [%]
2-A-1	1	347162000	358732789	3.33
2-A-2	0.8	389045600	407908543	4.85
2-A-3	0.6	434292000	481429079	10.85
2-A-4	0.5	457244000	437994830	-4.21
2-A-5	0	557056000	524090000	-5.92
2-B-1	1	294443600	272090000	-7,59
2-B-2	0.8	344190000	340112500	-1.18
2-B-3	0.6	409880000	453483333	4.50
2-B-4	0.5	418188000	521441333	24.7
2-B-5	0	533516000	524090000	1.77
2-C-1	1	216802800	164840000	-23.9
2-C-2	0.8	261571200	206050000	-21.2
2-C-3	0.6	324888400	274680000	-15.4
2-C-4	0.5	364371200	329680000	-9.5
2-C-5	0	505964000	437100977	-13.6

6 Discussion

From Table 5, it can be seen that for beams with an 8000 mm span, most of the critical moments from the collapse analysis are close to the critical moment from DG-25. For beam with an 8000 mm span, elastic buckling formula governs the calculation of the critical moment and the results of collapse analysis also show that the stresses at peak load is still in elastic range. The difference of critical moments computed using the design guide and the collapse analysis is between -14.2% to 18.3%. The minus sign means that the DG-25 critical moment is less than critical moment in the collapse analysis. If it is assumed that the collapse analysis is the real one, minus sign means the DG-25 is on the safe side. For Beams 1-A-5 and 1-C-5 the difference is high and not on the safe side.

From Table 6, it can be seen that for beams with a 4000 mm span, the critical moment computed by the collapse analysis is generally greater than the critical moment of DG-25. The difference is between -23.9% to 24.7%. There is only one beam that the critical moments of DG-25 is higher and not on the safe side. For beams with a 4000 mm span, inelastic buckling formula governs the calculation of the critical moment. The result of the collapse analysis also shows that the stresses at the peak load at the flange are in inelastic range.

It can be said that, the DG-25 is usually close to the collapse analysis and on the safe side, but sometimes it is higher and not on the safe side. Moreover the critical moment for the long beam using design guide is more accurate than for the short beam.

7 Conclusion

The collapse analysis have been made on a series of web-tapered beams and the conclusions drawn from this study are,

1. The critical moment for the long beam which is computed by elastic buckling formula of DG25 is usually close to the collapse analysis but sometimes it is higher and not on the safe side.
2. The critical moment for the long beam which is computed by DG25 is more accurate than the critical moment for the short beam.

The authors wish to thank Parahyangan Catholic University for its permission to use the licensed Adina Program.

References

1. D. Polyzois, I.G. Raftoyiannis, J. Of Struct. Eng. , 124, 1208-1216 (1998)
2. B.S. Miller, Thesis, Univ. of Pittsburgh, (2002)
3. J.S. Park, J. M. Stalling, J. Of Struct. Eng. , **129** 1457-1465, (2003)
4. T. Vandermeulen, J.P. Jaspart, N. Boissonnade, 5th Int.Conf. on Adv. In Steel Struct., Singapore, (2007).
5. L. Zhang, G. S., Tong, J. Constr. Steel Research, **64**, 1379-1393, (2008)
6. I.G. Raftoyiannis, T. Adamakos, Op. Constr. And Build. Tech. J. E **4**, 105-112, (2010)
7. M. Kovac, Procedia Engineering, **40** , 217-222, (2012).
8. Naaim N, F. De'nan, K.K. Choong, F. Azar, MAT. Web of Conf. , **47** (2016)
9. T. Patil, N.L. Shelke, J. Of Steel Struc. And Constr., **2 :2** (2016)
10. R.C. Kaehler, AISC Design Guide 25. (2011)